

# Development of Barium-doped Lead Magnesium Niobate-based Ceramics

A. Ahmad<sup>1\*</sup>, A.G. McDonald<sup>1</sup>, S.E. Prasad<sup>2</sup> and R.G. Blacow<sup>2</sup>

<sup>1</sup>Materials Technology Laboratory, Natural Resources Canada  
3484 Limebank Road, Ottawa, Ontario, Canada K1A 0E4  
[aaahmad@nrcan.gc.ca](mailto:aaahmad@nrcan.gc.ca)

<sup>2</sup>Sensor Technology Ltd.  
P.O. Box 97, 27 Stewart Road, Collingwood Ontario, L9Y 3Z4  
[epasad@sensortech.ca](mailto:epasad@sensortech.ca)

## ABSTRACT

Precursor powders of lead magnesium niobate-lead titanate-based ceramics doped with 2 weight % excess PbO, 2-4 weight % excess MgO and 0 or 1 mole % BaTiO<sub>3</sub>, were synthesized via a low-cost attrition milling process. The powders were calcined at 850°C for 2 hrs, re-attrition milled, formed into discs via uniaxial pressing and fired at high temperatures using various sintering temperature-sintering time profiles. The influence of powder composition and sintering conditions on the densification, microstructure and phase composition, as well as on the dielectric and electromechanical properties, was investigated. The data indicates that the above properties of the sintered discs are strongly influenced by the material composition and the sintering conditions used to produce the sintered discs.

**Keywords:** Piezoelectric, Electrostrictive, Materials, Processing, Properties, Taguchi Statistical Design for Experiments

## INTRODUCTION

The high dielectric constant and excellent, piezoelectric and electrostrictive properties of the lead-based perovskite ferroelectric and relaxor ferroelectric ceramics make them attractive for a variety of electromechanical sensor, actuator and transducer applications, including industrial process control (1-4). The complex perovskites, lead magnesium niobate ( $\text{Pb}(\text{Mg}_{1/3}\text{Nb}_{2/3})\text{O}_3$  or PMN), lead titanate ( $\text{PbTiO}_3$  or PT) and lead zirconate titanate ( $\text{Pb}(\text{Zr}_{(1-x)}\text{Ti}_x)\text{O}_3$  or PZT) and their solid solutions exhibit superior dielectric and electromechanical characteristics, particularly near their morphotropic phase boundary (MPB). PZT materials near the tetragonal-rhombohedral MPB display very interesting piezoelectric properties and have been widely used for over 40 years for various sensor and actuator applications. PMN is a relaxor ferroelectric, characterized by strong frequency dependent dielectric maxima ( $T_m$ ) around  $-10^\circ\text{C}$  and a diffuse phase transition, whereas PT and PZT are typical ordered ferroelectrics and exhibit a sharp phase transition peak. PMN has a high dielectric constant and substantial electrostrictive coefficient that make it attractive for capacitor and actuator applications (6-8). PMN is known to easily form solid solutions (8) with PT ( $T_m \sim 490^\circ\text{C}$ ). The piezoelectric properties of PMN can be enhanced through addition of PT. The PMN-PT solid solutions with approximately 30-35% PT exhibit a MPB and large piezoelectric properties (5, 10-11) and compositions with  $\text{PT} < 0.2$  have been studied for electrostrictive applications (3). It is known that the dielectric and piezoelectric properties of PMN or PZT ceramics can be improved by doping the material with various isovalent, monovalent and trivalent cations at the lead site (12-15). This paper provides the preliminary results of our investigations on the influence of materials and processing conditions on the microstructure/phase composition and dielectric and electromechanical properties (e.g., strain, hysteresis) of the PMN-PT based ceramics [ $0.87\text{Pb}(\text{Mg}_{1/3}\text{Nb}_{2/3})\text{O}_3 - 0.13(\text{PbTiO}_3)$ ] doped with or without 0.01 mole%  $\text{BaTiO}_3$ .

The study also involves the use of Statistical Design for Experiments (SDE) methodology developed by Genichi Taguchi (16-18) to optimize the process of engineering experimentation. SDE is a powerful statistical technique introduced by Sir Ronald Fisher in England in the 1920's for the agricultural industry to study the effect of multiple factors simultaneously on the quality of crop production. Since that time, much development has taken place in SDE area. In a classical SDE technique, one investigates all possible interactions (i.e., a full-factorial design). This could be very time-consuming and expensive. For example, in order to investigate seven factors at two levels, one must conduct  $2^7 = 128$  experiments under a full-factorial design. The Taguchi design approach provides an economical alternative by utilizing only a small portion of the full factorial array to study the main factors, noise or un-controllable factors and some of the factor interactions. The Taguchi SDE approach can be used to identify the best/optimum condition for a product or process, estimate the influence of individual factors as well as predict the product performance under optimum processing conditions. Perhaps the Taguchi's most significant contribution to SDE methodology is the development of simple standardized "orthogonal arrays" that can be used for a number of experimental situations. The Materials Technology Laboratory at NRCan has been using SDE methodology for the process/product design for over 15 years. In our experience, SDE is the most systematic way to plan, conduct, analyze and interpret experimental data. For details on Taguchi methodology, please see references (16-18).

## MATERIALS AND METHODS

The following are the elemental compositions of the powders used in this study:

Powder/Material	Elemental Composition
A	$[0.87\text{Pb}(\text{Mg}_{1/3}\text{Nb}_{2/3})\text{O}_3 - 0.13(\text{PbTiO}_3)]$
B	$0.99[0.87\text{Pb}(\text{Mg}_{1/3}\text{Nb}_{2/3})\text{O}_3 - 0.13(\text{PbTiO}_3)] - 0.01[\text{BaTiO}_3]$

The above compositions contained 2 Wt % of excess PbO, to potentially compensate for PbO loss at high sintering temperatures. The powders were prepared by conventional mixed oxide method via attrition milling of the reagent grade precursor raw materials using zirconia milling media in water. The processing factors and their levels selected in this study to generate a Taguchi  $L_8$  orthogonal array matrix are shown in Table 1. A full factorial design would require 32 experiments to investigate all of the factor interactions. Eight different experimental/trial conditions were produced (see Table 2) using Taguchi experimental design software obtained from Nutek Inc., USA. As shown below in Table 1, (2-4 wt %) MgO in excess of stoichiometric composition was used as one of the process variables. Previous work in our lab and elsewhere has shown that excess MgO helps in stabilizing crystal structure (i.e., reduces pyrochlore phase formation) and improves dielectric and electromechanical properties of the PMN-based ceramics. The powders were calcined at 850°C for 2 hrs. Discs were formed by uniaxial pressing of the calcined powders using a PVA binder and sintered at various temperatures. The density of the sintered samples was calculated by measuring the mass and the volume of the discs. X-ray diffractometry was used to analyze the phase compositions of the sintered parallel-lapped (using 600 grit SiC) discs. The major peak intensities of the perovskite (Pr, 110) and pyrochlore (Py, 222) phases were measured and the percentage of the pyrochlore phase was calculated using the following equation:

$$\% \text{Py} = 100 \times I(\text{Py}) / [I(\text{Py}) + I(\text{Pr})] \quad (1)$$

For dielectric property measurements, the sintered samples were electroded (using Dupont #4731 silver ink). The electrodes were fired at 600°C for 15 minutes. The dielectric constant and dielectric loss data were obtained at room temperature at a frequency of 1 kHz using an HP-4194A impedance analyzer. Strain and hysteresis measurements were realized by subjecting the samples to an ac electric field of 1MV/m, at a period of one second, while examining the displacement using LVDT (Schavitz Model 050-HP), driven by a lock-in amplifier (Standard Research System Model 830). The % strain and % hysteresis were calculated using the following relationships:

$$\% \text{ Strain} = (\text{Maximum Displacement}/\text{Sample Thickness}) * 100$$

$$\% \text{ Hysteresis} = (\text{Separation Between Curves at Half Field}/\text{Maximum Displacement}) * 100$$

**Table 1: Process factors and levels used to generate Taguchi design matrix**

Process Factors	Level 1	Level 2	Level 3	Level 4
Sintering Temperature	1180°C	1200°C	1220°C	1250°C
Sintering Time	2 hrs	4 hrs		
Wt% excess MgO	2 wt %	4 wt %		
BaTiO3	0 mole%	1 mole%		

**Table 2: Factors matrix/trial conditions produced using Taguchi design approach**

TC# (Trial Condition #)	Sintering Temperature	Sintering Time	Excess MgO	BaTiO <sub>3</sub>
1	1180°C	2 hrs	2 wt %	0 mole %
2	1180°C	4 hrs	4 wt%	0.01 mole%
3	1200°C	2 hrs	2 wt%	0.01 mole %
4	1200°C	4 hrs	4 wt%	0.0 mole%
5	1220°C	2 hrs	4 wt%	0.0 mole %
6	1220°C	4 hrs	2 wt%	0.01 mole%
7	1250°C	2 hrs	4 wt%	0.01 mole %
8	1250°C	4 hrs	2 wt%	0.0 mole%

## RESULTS AND DISCUSSION

The response/characteristics of the samples processed using eight different experimental/trial conditions, is summarized in Table 3. The measured density of the samples displayed only a slight dependence on the trial conditions. The samples exhibited relatively large dielectric loss values ( $>0.04$ ). In general the data indicates that the various performance characteristics are significantly influenced by the processing conditions as well as powder composition used to fabricate the samples. Fig. 1 shows a typical example of an x-ray diffraction (XRD) pattern of the sintered and parallel-lapped discs. The concentration of the pyrochlore phase varied significantly (from 0.01-7.87) under different processing conditions. Since the pyrochlore phase is known to deteriorate the dielectric properties of the PMN based materials, a small or preferably no pyrochlore phase is desirable. To determine the optimum processing condition for each performance characteristic, the average performance is computed for each process factor and plotted for a visual inspection using the Nutek software. Fig. 2 shows the effect of sintering time, mole% BaTiO<sub>3</sub> and wt% excess MgO on the concentration of the pyrochlore phase. The graph indicates that to minimize the formation of pyrochlore phase, the sintering time and mole% BaTiO<sub>3</sub> should be kept at lower level (i.e., level 1, 2hrs and 0 mole% respectively) and wt % MgO should be kept at level 2 (i.e. 4 wt %). A sintering temperature of 1220°C (level 3) was also favourable in lowering % Pyrochlore (Fig. 8). Statistical calculations based on the Analysis of Variance (ANOVA) methodology were performed on the experimental data using Nutek software to determine the % contribution or influence of each process factor on the pyrochlore phase formation (Fig. 3). It was found that sintering temperature, mole% BaTiO<sub>3</sub> significantly contributed to lowering of the pyrochlore phase (% Pyro), while wt% MgO displayed relatively smaller influence on % Pyro. The statistical analysis of the data also projected that % pyrochlore phase can be eliminated under optimum processing conditions. Figs. 4-8 provide similar statistical data analysis on the dielectric constant and % Strain.

The magnitude and shape of electrically-induced strain/hysteresis curves for the samples were also significantly influenced by the processing conditions (see Table 3). These results are not discussed here due to the size limitation guideline for the publication, but will be discussed in detail during the presentation. The optimum performance conditions and the projected performance under the optimum conditions for various response characteristics are given in Table 4 below. Confirmatory tests on samples processed under optimum conditions provided  $K^T$  values close to that projected by the statistical data analysis.

**Table 3: Effect of experimental/trial conditions on physical properties**

Trial Condition #	Density g/cc	% Pyro Phase	$K^T$ @1KHz, 25°C	Loss Tan $\delta$	Strain %	Hysteresis %
1	7.74	5.07	6285	0.048	0.047	39.0
2	7.81	7.87	6475	0.051	0.034	37.0
3	7.82	4.92	7512	0.053	0.042	39.0
4	7.95	0.30	6683	0.055	0.075	74.0
5	8.19	0.01	7950	0.045	0.068	110.0
6	8.07	3.90	8882	0.058	0.036	51.0
7	7.93	3.56	7696	0.056	0.039	39.0
8	8.14	2.99	9080	0.057	0.055	52.0

$K^T$ = dielectric constant (at 25°C ), tan  $\delta$  = dielectric loss

**Table 4. Optimum processing conditions based on statistical analysis of results/data.**

Property	Predicted Optimum Conditions, Level				Projected Performance
	Sint. Temp.	Sint. Time	Wt % excess MgO	Mole % BaTiO <sub>3</sub>	
Density g/cc	1220°C, L3	4 hrs, L2	4, L2	0.0, L1	8.20
% Pyro	1220°C, L3	2 hrs, L1	4, L2	0.0, L1	0.0%
$K^T$ (poled)	1250°C, L4	4 hrs, L2	2, L1	0.01, L2	9140
Loss tan $\delta$	1180°C, L1	2 hrs, L1	4, L2	0.0, L1	0.044
Strain %	1200°C, L2	4 hrs, L2	2, L1	0.01, L2	0.075
Hysteresis	1180°C, L1	4 hrs, L2	2, L1	0.01, L2	13%

### CONCLUSIONS/SUMMARY

The results show that the processing factors and their levels selected for various experimental conditions using Taguchi SDE methodology significantly influenced the performance of the PMN-PT based ceramics used in this study. The dielectric constant of the materials varied from 6285 to 9080 depending on the processing condition. Similarly, electrically-induced % strain of the samples varied from (0.036-0.075%) depending on the material composition and the processing conditions. The % Pyrochlore phase formation as well as the shape and magnitude of the electrically-induced strain/hysteresis curves were also considerably influenced by the process factors. The SDE methodology not only identified which factors and their levels (e.g., high/low) are important in optimizing the physical properties of the samples, but also provided information on the % contribution of each process factor to the properties of these materials. The purpose of this preliminary investigation was to determine the influence of various processing factors using SDE methodology. The preliminary results are very encouraging. Further work is planned to study the influence of temperature and frequency on the dielectric and piezoelectric properties of these materials.

## REFERENCES

1. Hana, P., Marvan, M., Burianova, L., Zhang, S.J, Furman, E and Shrout, T.R, “ Study of the Inverse Flexoelectric Phenomenon in Ceramic Lead Magnesium Niobate-Lead Titanate”, *Ferroelectrics*, 336: 137-144, 2006.
2. Wadhwan, V.K., Pandit, P., Gupta, S.M., “PMN-PT based relaxor ferroelectrics as very smart materials”, *Material Science and Engineering B* 120 (2005) 199-205.
3. Viehland, D., Li, Jie-Feng, McLaughlin, E., Powers, J., Janus, R., Robinsin, H., “Effect of uniaxial stress on the large-signal electromechanical properties of electrostrictive and piezoelectric lead magnesium niobate lead titanate ceramics”, *J. Applied Physics* 95, 4, (2004) 1969-1972.
4. Babooram, K., Ye, Z.G., “Polyethylene Glycol-Based New Solution Route to Relaxor Ferroelectric  $0.65\text{Pb}(\text{Mg}_{1/3}\text{Nb}_{2/3})\text{O}_3-0.35\text{PbTiO}_3$ ”, *Chem. Mater.* 2004, 16, 5365-5371.
5. Winter, M.R., Pilgrim, S.M., “Study on the Effect of Lanthanum Doping on the Microstructure and Dielectric Properties of  $0.9\text{Pb}(\text{Mg}_{1/3}\text{Nb}_{2/3})\text{O}_3-0.1\text{PbTiO}_3$ ”, *J.Am.Ceram. Soc.* 84[2] 314-20, 2001.
6. Shrout, R., Halliyal, A., “Preparation of Lead-based Ferroelectric Relaxors for Capacitors”, *Am. Ceram. Soc. Bull.*, 66[4] 704-11, 1987.
7. Jang, S.J., Nomura, S., and Cross, L.E., “Electrostrictive Behavior of Lead Magnesium Niobate Based Ceramics”, *Ferroelectrics*, 27, 31-34, 1980.
8. Waechter, D.F., Liufu, D., Camirand, M., Blacow, R. G. and S.E. Prasad, "Development of high-strain low-hysteresis actuators using electrostrictive lead magnesium niobate (PMN)", *Proc. 3rd CanSmart Workshop on Smart Materials and Structures*", Montreal, September 28-29, 2000, pp.31-36.
9. Choi, S.W., Shrout, S.J. Jang, Bhalla, A., “ Morphotropic Phase Boundary in  $\text{Pb}(\text{Mg}_{1/3}\text{Nb}_{2/3})\text{O}_3-\text{PbTiO}_3$ ”, *Mater. Lett.* 8 (1989) 253-255.
10. Schmidt, G., *Phase Transitions* 20, 127 (1990)
11. Chen, Y-H, Hirose, S., Viehland, D., Uchino, K., Doping Effects in  $\text{Pb}(\text{Mg}_{1/3}\text{Nb}_{2/3})\text{O}_3-\text{PbTiO}_3$  Ceramics for High Power Transduction Applications”, *Mat. Res. Soc. Symp. Proc.* Vol.604, 215-220 (2000)
12. Yoon, K-H., Lee H.R., “Effect of  $\text{Ba}^{2+}$  Substitution on Dielectric and Electric-Field-Induced Strain Properties of PMN-PZ-PT Ceramics.
13. Chen, Y-H., Uchino, K., Viehland, D., “Substituent Effects in  $0.65\text{Pb}(\text{Mg}_{1/3}\text{Nb}_{2/3})\text{O}_3-0.35\text{PbTiO}_3$  Ceramics”, *J. Electroceramics*, 6:1, 13-19, 2001.
14. Kanai, H., Furukawa, O., Abe, H., and Yamashita, Y., “Dielectric Properties of  $(\text{Pb}_{1-x}\text{X}_x)(\text{Zr}_{0.7}\text{TiO}_{0.3})\text{O}_3$  (X = Ca, Sr, Ba,) Ceramics, *J. Amer. Ceram. Soc.*, 77 [10], 2620 (1994).
15. Li, J., Dai, X, Chow, A. and Viehland, D. “Polarization Switching Mechanisms and Electromechanical Properties of La-Modified Lead-zirconate Titanate Ceramics”, *J. Mater. Res.* 10 [4] 926, (1995).
16. Shaw, J. C., Lin, K. S. and Lin, I. N., “Dielectric behavior at morphotropic phase boundary for PMN–PZT ceramics”, *Scripta Mater.*, 1993, **29**, 981–986.
17. Taguchi, G., Chowdhury, S., Wu, Y, “Taguchi Quality Engineering Handbook”, John Wiley & Sons, Inc, New Jersey, USA (2005)
18. Taguchi, G., “System of Experimental Design: Engineering methods to optimize quality and minimize costs”, American Suppliers Institute, 1987.
19. Roy, R., “Design of Experiments Using Taguchi Approach: 16 Steps to Product and Process Improvement”, John Wiley & Sons, USA (2001).

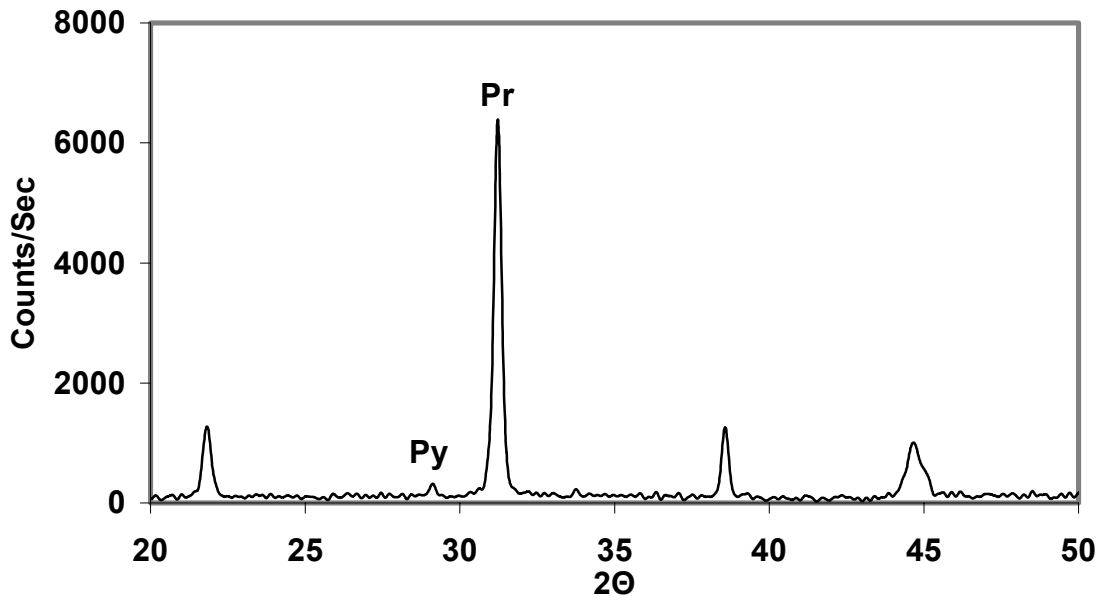


Fig.1. Typical XRD pattern for PMN-PT based sintered and parallel-lapped sample.

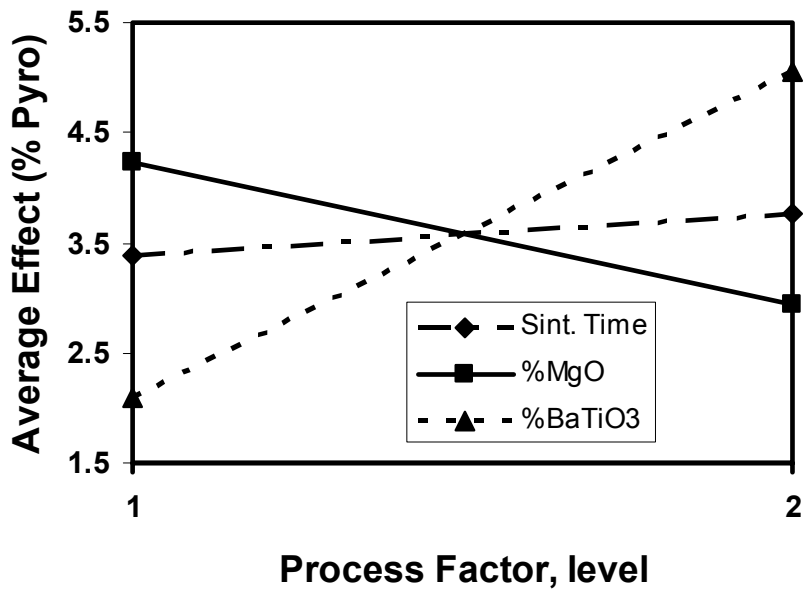


Fig. 2. Effect of process factors on % pyrochlore phase.

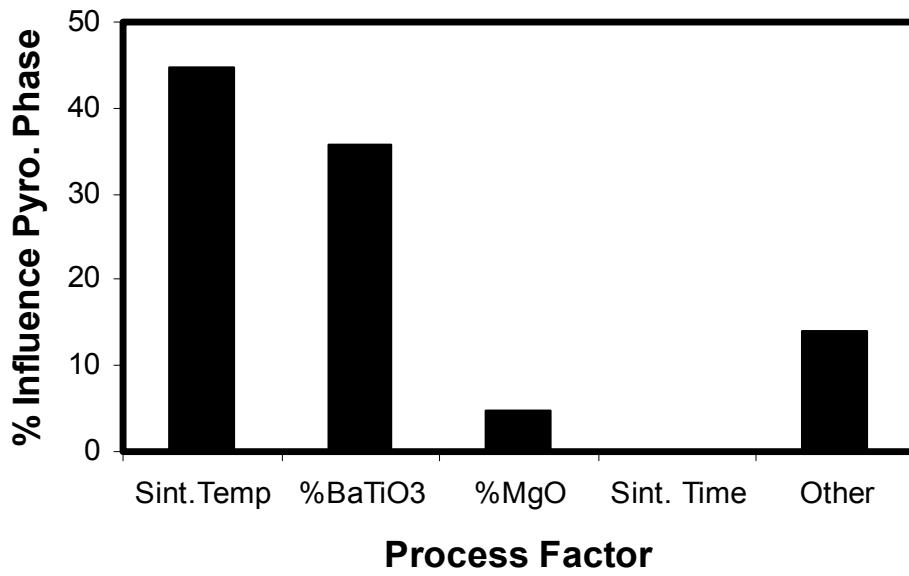


Fig. 3. % Influence of process factors on pyrochlore phase formation

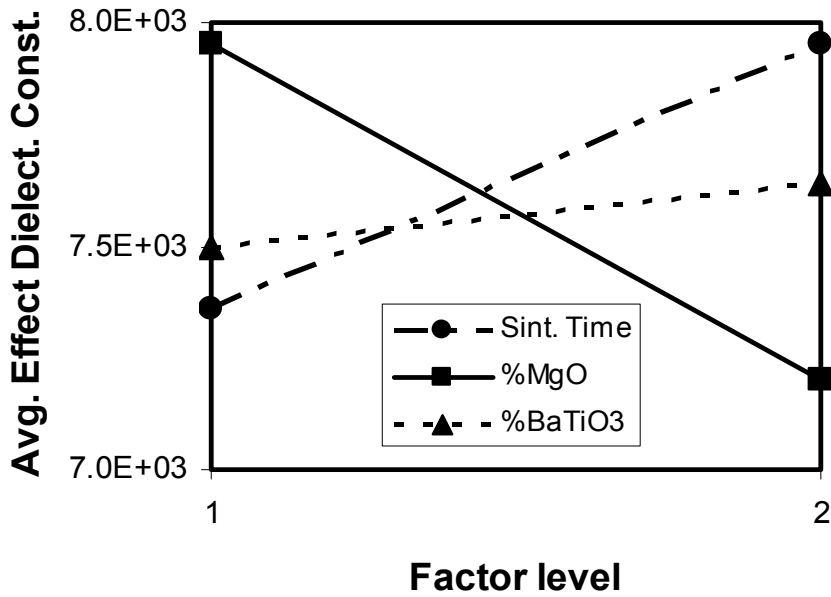


Fig. 4. Effect of process factors on  $K^T$ .



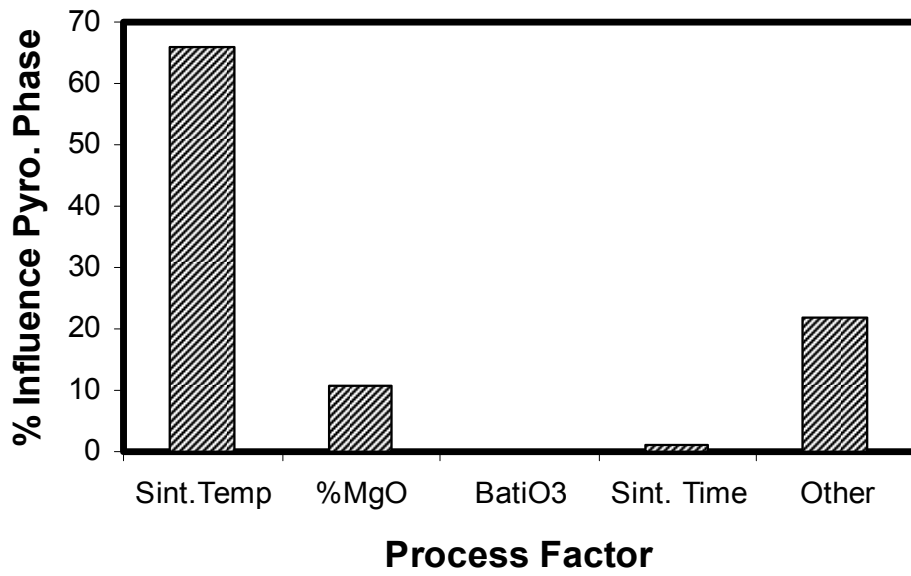


Fig. 5. % Influence of process factors on the dielectric constant ( $K^T$ ) of poled samples.

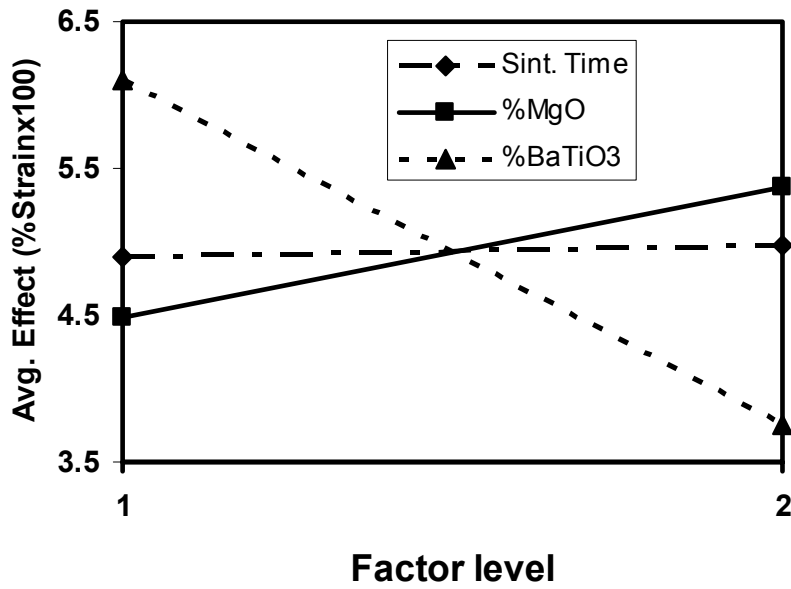


Fig. 6. Effect of process factors on % Strain @ 1MV/m

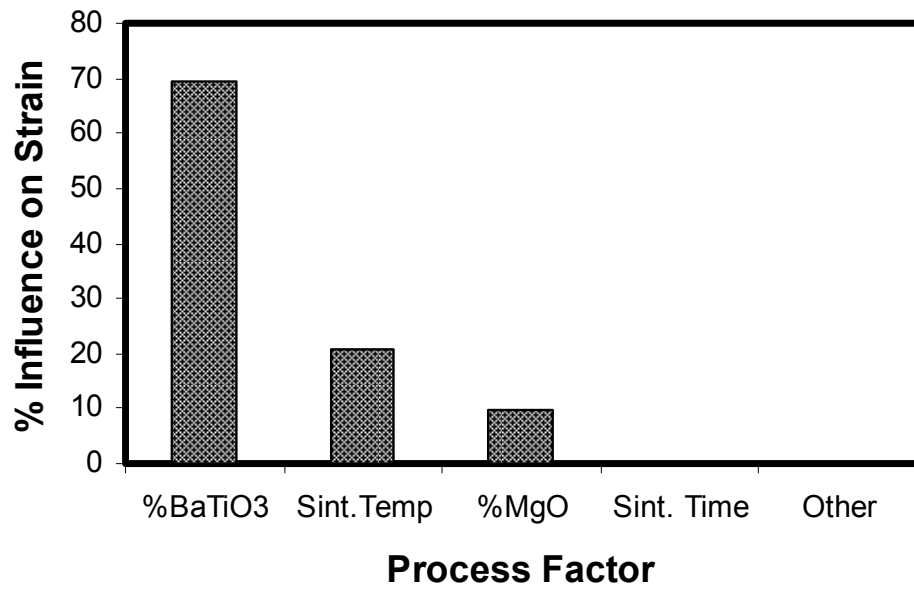


Fig. 7. % Influence of process factors on sample strain @ 1MV/m

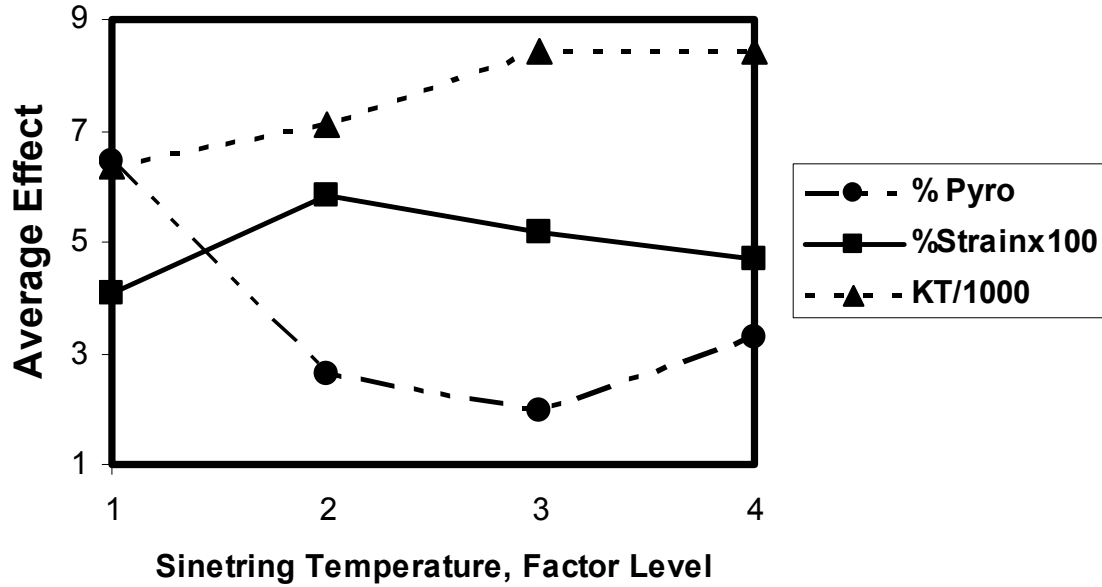


Fig. 8. Effect of sintering temperature on % pyro, % strain and dielectric constant  $K^T$ .